An Experimental Method to Measure Hemispherical Emissivity and Solar Absorbtivity of Space Flight Materials

Steen C. Vecchi
Colorado State University
Advisor: Dr. John Williams

ABSTRACT

In spacecrafts using electric propulsion thrusters, sputter products can deposit onto thermal control surfaces. In terms of thermal management, the deposited films can lead to changes in solar absorbtivity and hemispherical emittance of the thermal control surfaces. We investigate the effect of films of black kapton that are sputter deposited onto quartz substrates (radiator surfaces). We performed measurements of (changes in) solar absorbtivity and hemispherical emissivity for the aforementioned material for different values of film thickness. The solar absorbtivity measurements used a reflecting spectrophotometer, while hemispherical emissivity is measured with a calorimetric method. From these measurements we were able to show that as the coating thickness increased the emissivity of the samples also increased. The solar absorbtivity is also determinate of the thickness as the thickness increases the reflectivity goes down.

INTRODUCTION

Solar absorbtivity and emissivity values are critically important for validating temperature predictions of systems operated in a space flight environment. Solar absorbtivity is typically measured by recording the absorbtivity of a sample surface as a function of wavelength and convolution with the solar intensity.

One technique for measuring hemispherical emissivity involves the use of an assembly comprised of a heater sandwiched between two identical samples that are placed within a vacuum chamber. When the assembly is placed within a cooled cavity with an emissivity close to unity and power is supplied to the heater, one can calculate the sample emissivity from measurements of the sample temperature and the heater current and voltage.

The cooled cavity used in this study was fabricated from carbon black velvet to ensure the best possible black body simulation. Several tare errors exist in this type of measurement and include heat conduction and radiation from the thermocouple and power leads. Random errors include uncertainty in temperature measurement and heater current and voltage measurements. An uncertainty analysis is presented that documents the effects of the tare and random errors on the emissivity measurements.

TESTING SET-UP

All testing was conducted at Colorado State University's Ion Propulsion Laboratory using the vacuum chamber as shown in figure 1 below.

Figure 1: Testing Facilities

<u>CHAMBER SET-UP</u>

The chamber was first cleaned and then lined with 15 mil aluminum foil to keep sputtered particles off of the samples. A linear actuator was used to provide movement into and out of a black body cavity. The linear actuator is shown in figure 2.

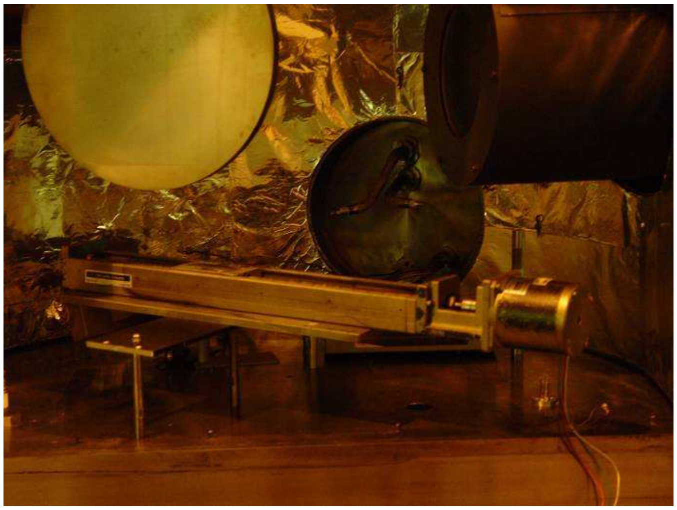

Figure 2: Linear Actuator for moving sample

The next step was to add a stepper motor for radial movement in order to move the sample into and out of the ion beam. This was necessary so that the beam would not be able to sputter material off of the samples. This is shown in Figure 3.

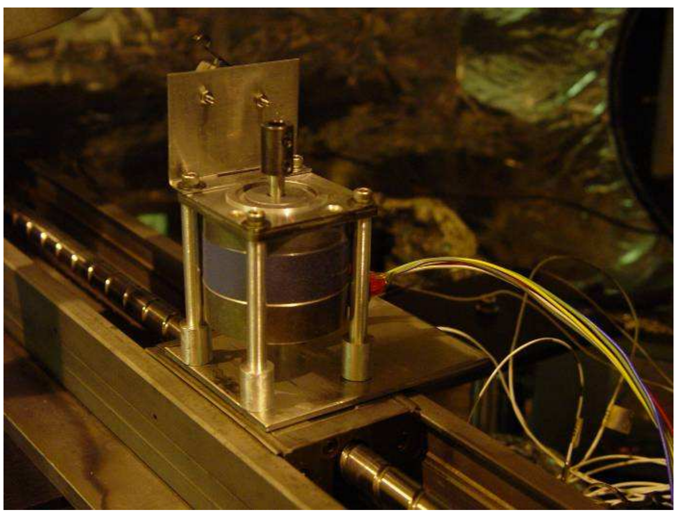

Figure 3: Stepper motor for rotational movement

We were next faced with a way to suspend the sample. A platform was created that would house the thermocouple connector, the lead wires and a leveling wire. It was also necessary to insure that the level wire was grounded; two ceramic insulating connectors were used for this. The platform was connected to an arm which is anchored to the stepper motor as in figure 4.

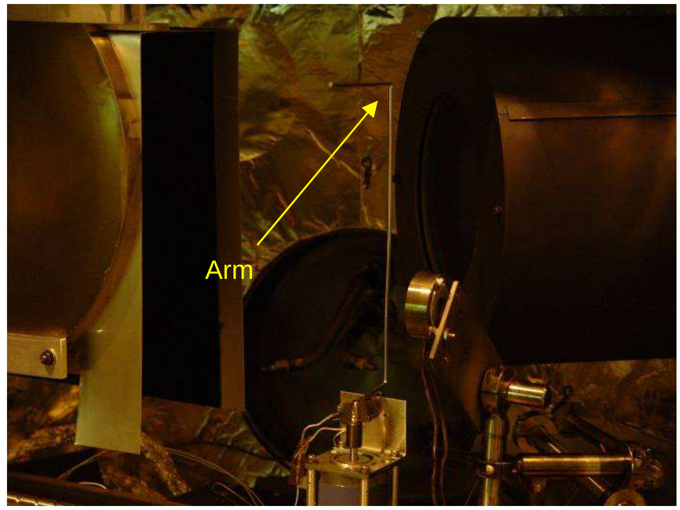

Figure 4: Stabilizing Arm

A QCM was then added to the initial setup. This allows us to determine the amount of mass sputtered onto the material. We have programmed into the Lab View files for the rotational motor to turn the sample out of the beam when the sample reaches a desired thickness. It was necessary to have the QCM and the sample in the same plane to ensure that the amount that was being sputtered onto the QCM was the amount being sputtered onto the sample.

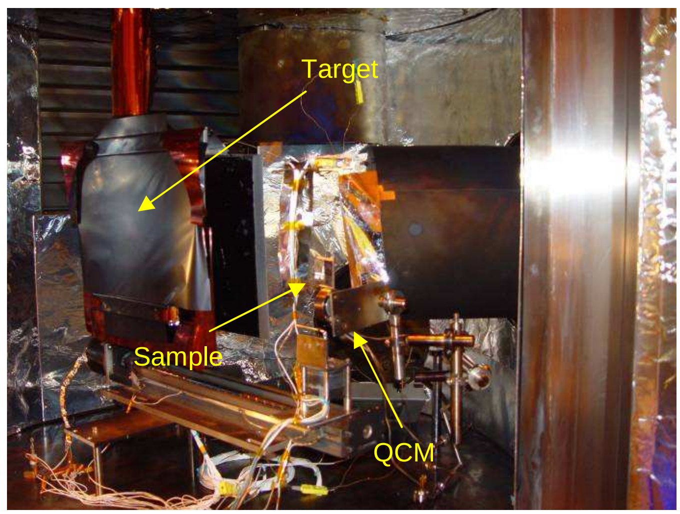

Figure 5: Symmetry of Sample and QCM

The target was then coated with the material to be sputtered. For these sets of experiments a black kapton sample was used. In order to ensure that the sample does not receive any errant sputtered materials, it was determined that we needed to keep the ion beam from being allowed to deviate from the target. For this reason wings were put on the target to envelope the entire beam; for the wings regular kapton was used. Regular kapton was used due to the fact that it has a very low sputtering rate. The final setup of the target is shown in figure 6.

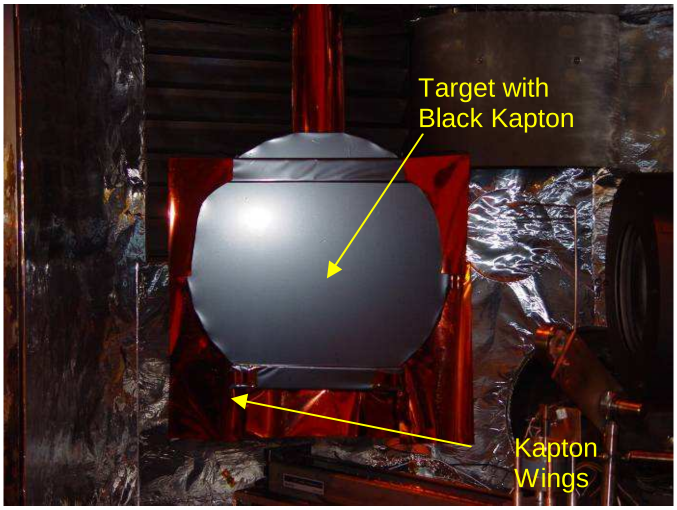

Figure 6: Target with Black Kapton Sputtering Material

In order to conduct the emissivity tests we needed to create a black body cavity. For this a black velvet was used which has an emissivity very close to unity. The cavity was attached to the target in such a way that the cavity would cool to the same temperature as the target. The target is maintained at 0 ℃ by an outside pump with a glycol and water mixture. We used convection in order to cool the cavity. We tried to create as much surface area contact with the target thus the size of the cavity. There is a six degree heat loss from the pump to the cavity. The sample is placed into the cavity as shown in figure 6. In this position all of the emissivity tests were conducted.

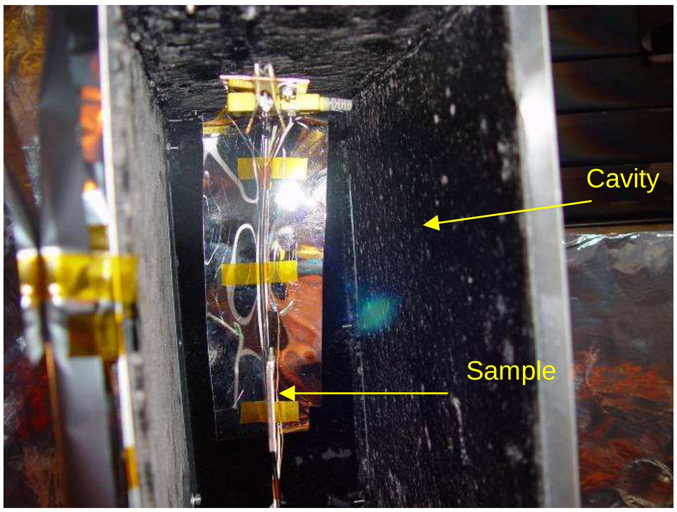

Figure 7: Sample inside Cavity

We have placed a thermocouple in the center of the backside of the cavity in order to make these temperature adjustments as shown in figure 8. With a thermocouple on the target and on the cavity we are able to make accurate temperature models of the emissivity.

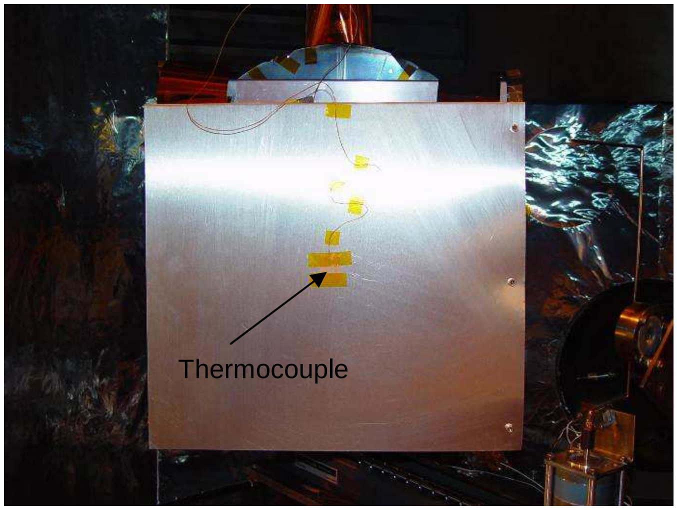

Figure 8: Thermocouple on Cavity Back

SAMPLE SET-UP

The samples were made up of three layers; a resistive heater with a thermocouple in the middle, a layer of copper and the quartz sample. The heater and thermocouple were sandwiched in-between the two pieces of 21 mil copper (43mm x 40mm). The copper layer was used as a heat spreader in order to maintain a constant temperature profile across the sample. The copper was then sandwiched in-between the sample. The sample was a piece of Quartz with an inconel coating measuring 40mm x 40mm. The copper was made larger due to the fact the heaters were made to accept a 43mm x 40mm sample. The components of the manufactured sample are shown in figure 9.

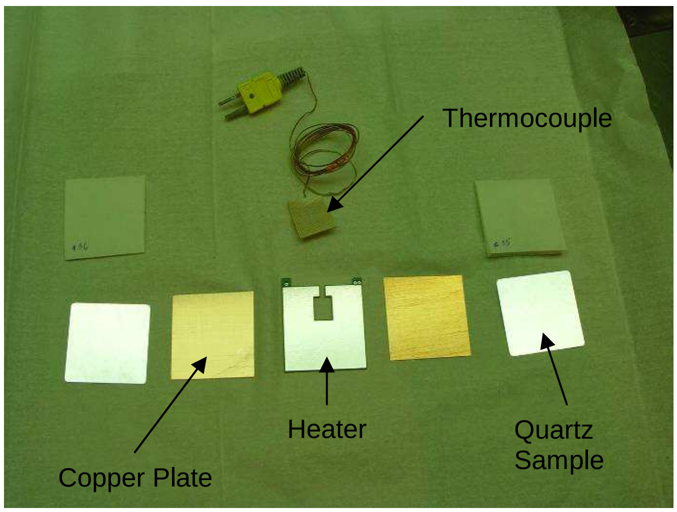

Figure 9: Sample Components

The thermocouple inside of the heater was needed in order to read the average temperatures of both sides of the sample. The heater was connected to an adjustable voltage supply via 30 gauge wire in order to help reduce the amount of error in the final emissivity calculations. The sample was supported by the heater lead wires, the thermocouple wires and the leveling wire. The final product looked like that of figure 10 below.

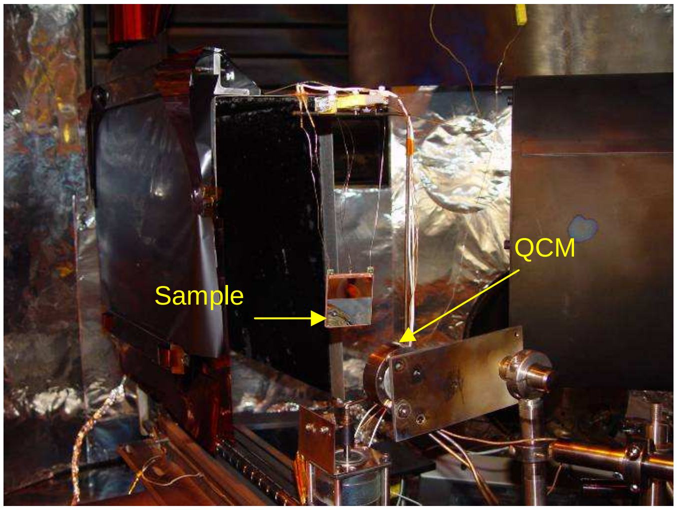

Figure 10: Sputtering Plane

TEST PROCEDURES

All tests were done at two different power levels: 1W and 2W. These power level values were chosen due to the unknown temperatures the heater would achieve. The thermocouples used were only rated to 250 ℃. The resistance of the heater was measured to be 20.4Ω. Thus the required voltages needed were 4.5V and 6.39V respectively. After the sample was coated the sample would then move into the black body cavity. Once the sample was inside the cavity, power to the heater would be activated and maintained at a constant voltage. The heater was then powered until it achieved a steady state level such as that shown in figure11. After the steady state was reached the temperatures of the cavity, the sample, the target and the vacuum chamber were recorded.

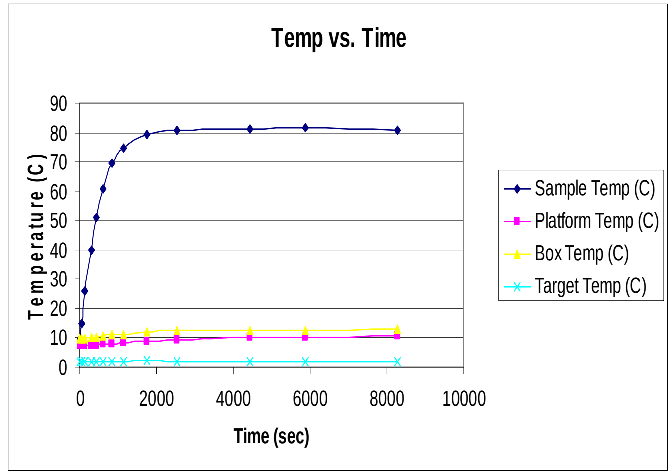

Figure 11: Temperature vs. Time

HEMISPHERICAL EMMISSIVITY CALCULATIONS

For the emissivity calculations the radiation equation shown in equation 1 was used.

$$P = \varepsilon\sigma A(T_s^4 - T_C^4)$$

Equation 1: Radiation Equation

With the power P, area A, the sample temperature T_s and the cavity temperature T_c known we are able to solve for the emissivity (ε). Because the cavity had two different temperatures one at the target and the other on the other side of the cavity, we needed to take this into account and modify the radiation equation to the form in equation 2.

$$P = \varepsilon\sigma A(T_S^4 - \frac{T_C^4}{2} - \frac{T_T^4}{2})$$

Equation 2: Radiation Equation with temperature corrections

Due to the fact that each side of the sample faced a different temperature source, this needed to be calculated into the findings. This was done by adding the two portions together and dividing the area by 2 like that in equation 3.

$$P = \varepsilon\sigma\frac{A}{2}\left(T_s^4 - T_C^4\right) + \varepsilon\sigma\frac{A}{2}\left(T_s^4 - T_T^4\right)$$

Equation 3: Temperature correction

The resulting equation being that of equation 2.

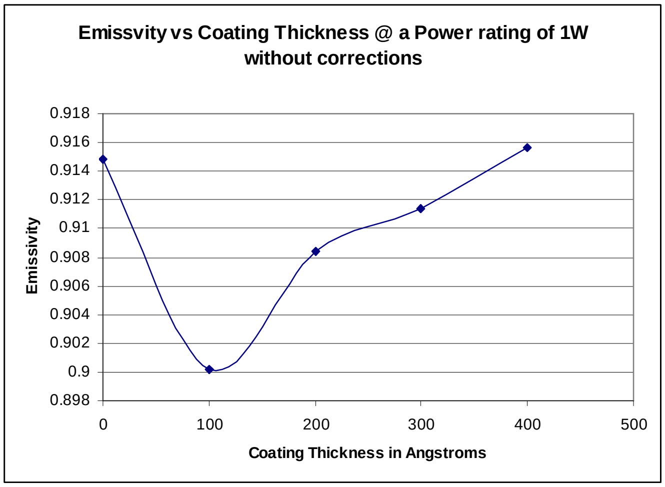

Figure 12: Graph Showing Emissivity w/out Corrections

From the above graph we see that the sample had an initial emissivity value of close to .91 which was higher than the expected values. There were expected errors in the readings therefore we needed to account for our tare error losses, addressed later. We also found something quite interesting, We found that at certain coating thicknesses the emissivity actually went down which was not an expected result for the sputtered material. The results that were expected were for the emissivity to stay constant or to rise slightly, which happens at thicker layers. At first this was believed to be an error in the testing procedure but after multiple samples this is a constant trend at 100Å even with different sample material such as copper.

SOLAR ABSORBTIVITY CALCULATIONS

In order for us to do the solar absorbtivity calculations the samples were taken to the chemistry department where we used their Cary 500 scan UV-Vis-NIR spectrophotometer using a variable angle specular reflectance accessory. With this apparatus we measured the percent reflectivity of the sample by scanning it through a range of wavelengths namely the 250 nm to 2000 nm range at a 30 degree incident angle.

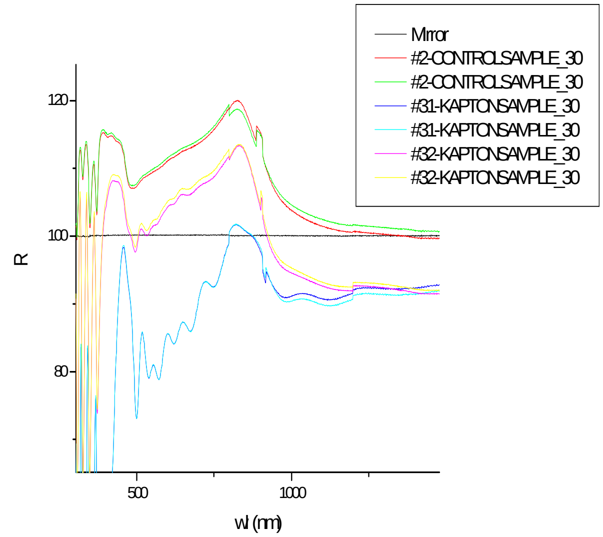

Figure 13: Graph of Reflectivity Values at Different Wave Lengths

The graph above shows two different samples with different sputter thicknesses and how their reflectivity changed due to coating thickness. As expected sample #31, the sample with the most sputtering had a larger decrease in reflectivity. After calculations were conducted we found that sample #31's reflectivity was 76% $\pm$ 1% and sample #32's reflectivity was 92% $\pm$ 1% of the control sample. We are able to find the solar absorbtivity for the samples by using the equation.

$$A_S = 1 - \%R$$

Equation 4: Solar Absorbtivity Equation

At the lower end of wavelength values we have a noise effect that gives us unreliable results. Exactly what is happening at the lower wavelengths has yet to be determined.

TARE ERROR CALCULATIONS

Due to the fact that we had other materials, such as the lead wires, and thermocouple wires, adding to the emissivity results, we needed to factor them into the calculations. We took into account the showing lead wires, thermocouple wires, the showing copper (top, bottom, sides and the 40mm x 3mm strip showing on the top of the sample), and the showing FR-4. We found the area of each of the pieces and then calculated the total power of each piece using equation 1. We were required to take into account the power due to conduction of the thermocouple and lead wires. For this we used a basic conduction equation as the one in equation 5.

$$P = \frac{\kappa A_C \Delta T}{l}$$

Equation 5: Conduction Equation

For the thermal conductivity constant of the lead wires we used a value for copper which is 400 $Wm^{-1}K^{-1}$. For the thermocouples which are alumel and chromel wires we used a value of 29 $Wm^{-1}K^{-1}$. This value was obtained from the manufactures. The chromel has a value of 17 $Wm^{-1}K^{-1}$ but we took the larger value for the conductivity constant due to the larger value and larger effect that it has on error loss.

For the copper we used an emissivity value of .1 which in later tests was determined to be .08. For the FR-4 we took an emissivity value of .8. We then took these power values for each piece and subtracted from equation 2, resulting in a new equation which was used to find the emissivity of the quartz samples.

$$\varepsilon = \frac{P - \sum P_{parts}}{2\sigma A(T_S^4 - \frac{T_C^4}{2} - \frac{T_T^4}{2})}$$

Equation 6: Modified Radiation Equation with Tare Errors Introduced

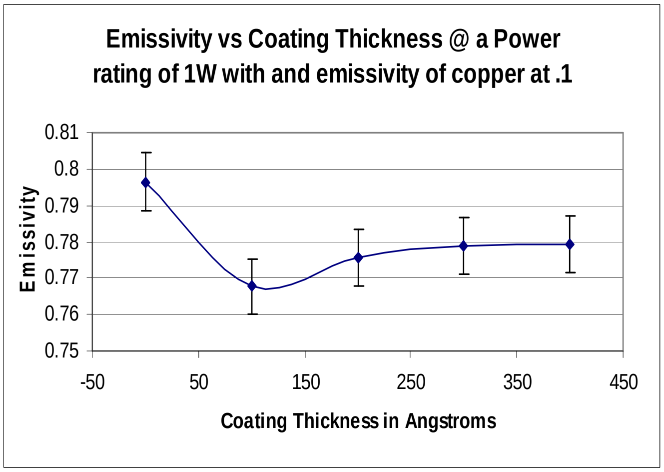

Figure 14: Emissivity Graph after Error Calculations

From the graph we see the corrections reduced the emissivity by more than 10 percent to a value of around .8 which where initial emissivity values of the obtained samples.

When plotted against each other we see that the two graphs match up well, however there is some noise error in the two graphs.

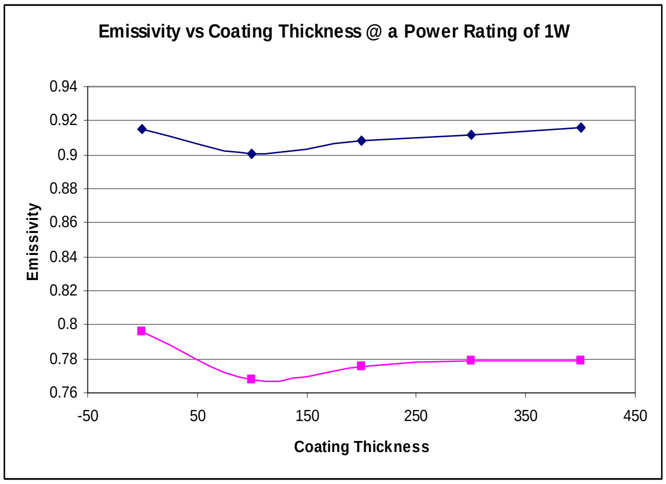

Figure 15: Tare Error vs. Non Tare Error Emissivity

There are still possible errors in the equations; we have an area that is showing to the chamber which has a different temperature than that of the black body cavity. This has not been factored in due to the fact that it is a negligible effect. There is also believed to be too much space in between the cavity and the sample that we may be losing some temperature effects to the cavity. As we take into account more of the errors we are able to decrease the uncertainty in the values that we have obtained for the emissivty and solar absorbtivity.

CONCLUSION

An investigation into the changes of solar absorbtivity and hemispherical emittance of a thermal control surface has been conducted.

A test facility was constructed on site in order to be able to test and record these values. Initial measurements found that the emissivity decreased at small values of coating and then increased as the coating thickness increased.

Investigation found that there was a large error due to tare errors due to heat radiated from the sample and heat conducted through the thermocouple and lead wires. Further calculations later introduced took into account these known causes, during the investigation random errors have been found and addressed.

From these measurements power sources for spacecrafts will be able to be better optimized and thermal management of satellites will be able to be modeled more effectively.

ACKNOWLEDGMENTS

Dr. John Williams, Colorado State University

Dr. Azer Yalin, Colorado State University

Dr. Hiroshi Sakurai, Colorado State University

Dr. Sandeep Kohli, Colorado State University

Mr. Casey Farnell, Colorado State University

Mrs. Daisy Williams, Colorado State University

Mr. Curtis Stovall, Colorado State University

Mr. Ron Corey, Space Systems Loral

Mr. Randy Pon, Space Systems Loral

REFERENCES

K. Fukuzawa, A. Ohnishi, and Y. Nagasaka, *The Total Hemispherical Emittance of Polymide Films for Space Use in the Temperature Range 173 K to 700 K,*

John E. Francis and Tom J. Love Jr., *Radiant Heat-Transfer analysis of Isothermal Diathermanous Coatings on a Conductor,* AIAA Journal, Vol. 4, No. 4 (April 1966) pp. 643-650

J. O. Isard, *The Emission of Thermal Radiation from Hot Glass. Part 1. Emissivity of Sheets, Spheres, Cylinders, and Tubes,* Glass Technology, Vol. 27, No.1 (February 1986) pp. 24-31

A. Galdikas, L. Pranevičius, and C. Templier, *Mass Transport Processes Initiated in Multielemental Solids Affected by Ion Beam Irradiation,* Surface Science, 349, (1996) pp. 333-341

E. R. Schleiger, *Measurement of Total Hemispherical Emittance of Transparent Materials at Low Temperature,* Applied Optics, Vol. 6, No. 5, (May 1967) pp. 919-923

Raakesh Raman and Alok Thakur, *Thermal Emissivity of Materials,* Applied Energy, 12, (1982) pp. 205-220

R. H. Munis and S. J. Marshall, *Thermal Emissivity of Diathermanous Materials,* Optical Engineering, Vol. 24, No. 5, (1985) pp. 872-878

CONTACT

Steen C. Vecchi

svecchi@msn.com

Definitions, Acronyms, Abbreviations

P = Power

A = Area

T_s = Temperature of the Sample

T_c = Temperature of the cavity

ε = emissivity

σ = Stefan-Boltzman constant

T_T = Temperature of the Target

ΣP_{parts} = Sum of all the tare error Powers

A_s = Solar Absorbtivity

%R = Reflective percentage

κ = Thermal conductivity

A_c = Cross sectional Area

l = Length of the wire

ΔT = Change in temperature

APPENDIX

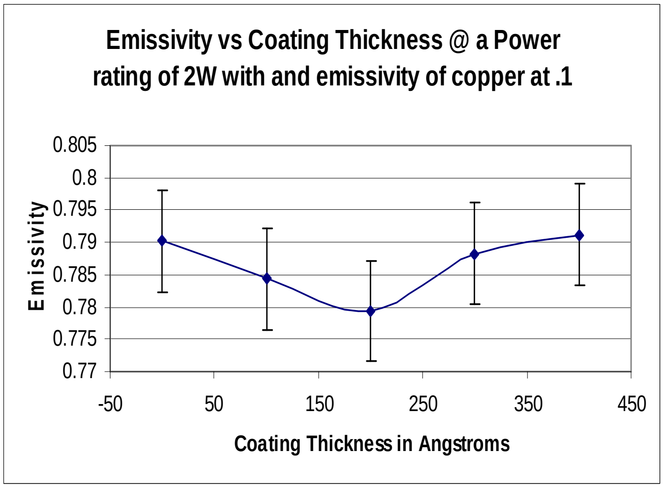

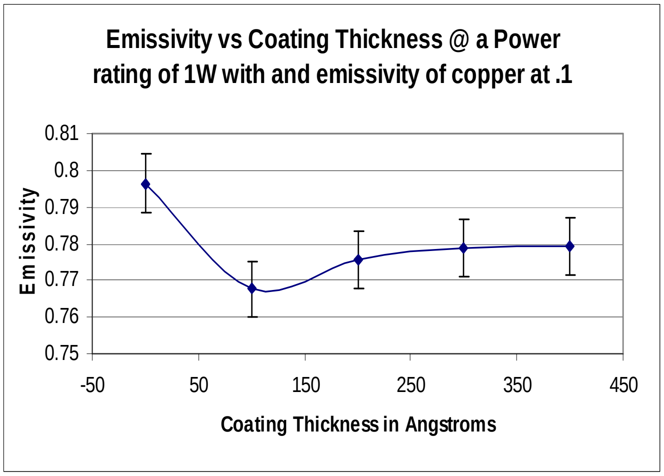

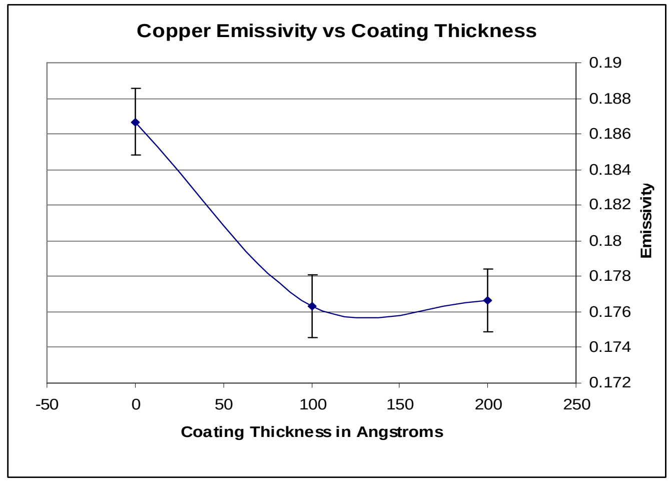

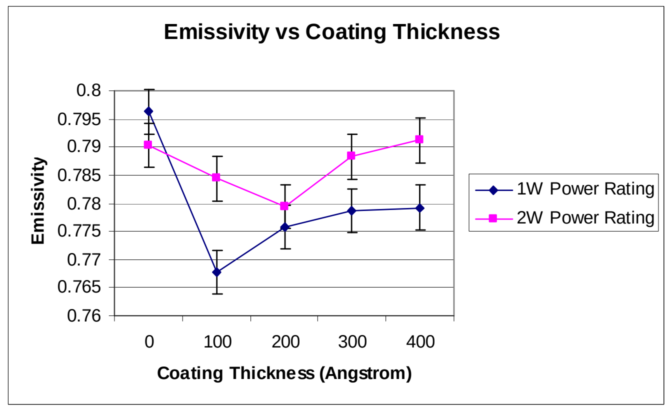

Area of copper face
0.00012 m

Area of copper top
0.000021336 m

Area of copper side
2.29362E-05 m

	Effects of FR-4 Assuming ε of .8
Tabs	0.019964872
Top	0.013763434
Bottom	0.013694842
Sides	0.031258724
Tab Sides	0.006499488

cond T/C	0.00097601
cond Cu	0.013462204

Area of showing FR-4	
Face of tabs	
2.12335E-05	m
Sides	
7.31774E-05	m
Top	
6.4441E-05	m
Bottom	
0.000068072	m
Tab Sides	
7.60773E-06	m

	Effects of copper Assuming ε of .1
front	0.007051899
sides	0.002449378
Top/bot	0.002278491